Inelastic collisions of CaCl(X 2Σ+) with Ar: A collaborative theoretical and experimental study

Millard H. Alexander, Stephen L. Davis, and Paul J. Dagdigian

Citation: The Journal of Chemical Physics **83**, 556 (1985); doi: 10.1063/1.449521
View online: http://dx.doi.org/10.1063/1.449521
View Table of Contents: http://scitation.aip.org/content/aip/journal/jcp/83/2?ver=pdfcov
Published by the AIP Publishing

Inelastic collisions of CaCl($X\,^2\Sigma^+$) with Ar: A collaborative theoretical and experimental study

Millard H. Alexander
Department of Chemistry, University of Maryland, College Park, Maryland 20742

Stephen L. Davis
Department of Chemistry, George Mason University, Fairfax, Virginia 22030

Paul J. Dagdigian
Department of Chemistry, The Johns Hopkins University, Baltimore, Maryland 21218

(Received 21 March 1985, accepted 5 April 1985)

We investigate rotationally inelastic cross sections of CaCl($X\,^2\Sigma^+$) with Ar at a collision energy of 0.24 eV. Theoretical cross sections, determined by coupled states calculations based on an electron-gas description of the potential surface, are compared with experimental cross sections, determined in a molecular beam apparatus involving initial state selection by an electric quadrupole field and final state detection by laser-induced fluorescence. The agreement between theoretical and experimental cross sections is excellent, except for the $e \rightarrow e$ transitions with $\Delta N =$ even, which suggests a residual inaccuracy in the theoretical description of the second Legendre moment of the anisotropy in the potential. Both the theoretical and experimental cross sections clearly confirm a propensity toward conservation of the spectroscopic e/f label. The sets of experimental and theoretical cross sections can be well fit by the sudden scaling relation, although the entire set of base cross sections cannot be well represented by a simple power law.

I. INTRODUCTION

Recently, sophisticated molecular beam and laser double resonance techniques have allowed the state-resolved study of rotational energy transfer in collisions involving open-shell molecules in their ground electronic state. These include NO($X\,^2\Pi$),[1,2] OH($X\,^2\Pi$),[3,4] and CaCl($X\,^2\Sigma^+$).[5,6] Inelastic processes in these systems are richer in detail, as compared to collisions of closed shell molecules in $^1\Sigma^+$ electronic states, because of the fine structure superimposed on the manifold of rotational states, which reflects the coupling between the rotation of the nuclei and the electronic spin and orbital angular momenta. Along with the experimental work cited above[1–6] have appeared a number of papers[7–15] devoted to the development of the quantum description of inelastic collisions involving open-shell molecules. Our own work[11–13] has demonstrated that transitions between certain fine structure levels will be favored, in particular those in which the spectroscopic e/f label,[16] which is directly related to the parity of the wave function of the rotating molecule, is conserved. This propensity rule is clearly observed in our experimental studies of collisions of CaCl($X\,^2\Sigma^+$)[5,6] as well as in cell experiments involving various electronically excited molecules,[17–19] and in calculations[13] of cross sections for collisions of NO($X\,^2\Pi$).

In two recent papers[5,6] we have presented a new technique for the measurement of state-to-state rotationally inelastic cross sections involving collisions of CaCl($X\,^2\Sigma^+$). Here this technique is applied to the scattering of CaCl($X\,^2\Sigma^+$) with Ar. The resulting experimental cross sections are compared with theoretical values determined within the quantum coupled-states approximation[11,20–22] and based on an electron-gas[23] description[24] of the interaction potential. The organization of the present article is as follows: In Sec. II we present a review of the relevant scattering formalism. Explicit use will be made of the powerful spin-decoupling scheme introduced by Corey and McCourt[14] for collisions of molecules in Σ electronic states with nonzero spin. This is followed, in Secs. III and IV, respectively, by the description of the scattering calculations and the presentation and analysis of the theoretical cross sections. The experimental work is summarized in Sec. V, and the comparison with theory is made in Sec. VI. A brief conclusion follows. In the Appendix we discuss some subtle details concerning the intensity factors needed in the experimental studies for the conversion of CaCl fluorescence signals to rotational populations.

II. SCATTERING FORMALISM

In a Hund's case (a) description[25] the definite parity wave function of a rotating molecule in a $^2\Sigma^+$ electronic state is written as[11,26]

$$|JM\epsilon^2\Sigma^+\rangle = 2^{-1/2}[|JM\Sigma\rangle|\Sigma\rangle + \epsilon|JM-\Sigma\rangle|-\Sigma\rangle]. \quad (1)$$

Here J denotes the total angular momentum of the molecule (spin + rotational) with projection M and Σ along space- and molecule-fixed axes, respectively; $|\pm\Sigma\rangle$ designates the electronic wave function with Σ, which equals 1/2, denoting the projection of the electronic spin S ($S = 1/2$) along the molecular axis; and $|JM\Sigma\rangle$ designates the rotational wave functions with coordinate representation[26,27]

$$|JM\Sigma\rangle = [(2J+1)/4\pi]^{1/2} D^{J*}_{M\Sigma}(\alpha\beta 0). \quad (2)$$

Here the Euler angles refer to the space-fixed orientation of the diatomic, and we assume active rotations[27] following Brink and Satchler.[28] For a diatomic molecule the third Euler angle can be set equal to zero without loss of generality[26]; this has been done in Eq. (2) and the wave function normalized accordingly.

The symmetry index ϵ in Eq. (1) can take on the values

 0021-9606/85/140556-11$02.10

± 1. The parity of the wave functions in Eq. (1) is[27] $\epsilon(-1)^{J-1/2}$. In conventional spectroscopic notation[16] the $\epsilon = +1$ levels are labeled e and $\epsilon = -1$ levels are labeled f.

An alternative description of the rotational wave function of a $^2\Sigma^+$ molecule corresponds to Hund's case (b).[25] We have[29]

$$|JMN^2\Sigma^+\rangle = \sum_{M_N M_S} (NM_N SM_S|JM)\ |NM_N|M_S\rangle \quad (3)$$

Here $(\cdots|\cdot\ \cdot)$ is a Clebsch–Gordan coefficient[28]; $|M_S\rangle$ designates the electronic wave function with electronic spin projected now along a space fixed axis; and $|NM_N\rangle$ designates the wave function corresponding to the rotational motion of the nuclei with angular momentum N and space-fixed projection M_N. The rotational wave function is given by

$$|NM_N\rangle = [(2N+1)/4\pi]^{1/2}\ Y_{NM_N}(\beta\alpha). \quad (4)$$

The explicit relation between the case (a) and case (b) wave functions can be derived easily.[29] The relation between N and ϵ, for a given J, is[30]

$$N = J - \tfrac{1}{2}\epsilon, \quad (5)$$

so that the e-labeled spin-doublet levels ($\epsilon = +1$) correspond to $J = N + 1/2$, and the f-labeled levels ($\epsilon = -1$), to $J = N - 1/2$. For $N = 0$ only the $\epsilon = +1$, e level exists.

In our earlier description of collisions of molecules in $^2\Sigma^+$ electronic states with closed-shell spherical atoms,[11] the total scattering wave function was expanded in terms of products of the case (a) molecular wave functions [Eq. (1)] multiplied by wave functions describing the relative orbital motion, which were designated $|LM_L\rangle$. The product functions are eigenfunctions of the total angular momentum $\mathscr{J}$ and its space-fixed projection $\mathscr{M}$, namely

$$|JL\epsilon\mathscr{J}\mathscr{M}\rangle = \sum_{MM_L} (JMLM_L|\mathscr{J}\mathscr{M})\ |JM\epsilon^2\Sigma^+\rangle|LM_L\rangle. \quad (6)$$

The scattering T-matrix elements are indexed in $\mathscr{J}$ and in the initial and final values of J, L, and ϵ. Similarly, as was done by Dixon and Field,[31] the scattering wave function can be expanded in terms of products of the case (b) molecular wave functions [Eq. (3)] and the relative orbital angular momentum functions. The total-$\mathscr{J}$ functions of Eq. (6) are replaced by

$$|JLN\mathscr{J}\mathscr{M}\rangle = \sum_{MM_L} (JMLM_L|\mathscr{J}\mathscr{M})\ |JMN^2\Sigma^+\rangle|LM_L\rangle, \quad (7)$$

with the T-matrix elements now indexed in $\mathscr{J}$ and in the initial and final values of J, L, and N. The vector coupling implicit in Eq. (7) may be represented by the two vector equations[14]

$$\mathbf{N} + \mathbf{S} = \mathbf{J} \qquad \mathbf{J} + \mathbf{L} = \mathscr{J}. \quad (8)$$

In an important recent development Corey and McCourt[14] suggested an alternative coupling scheme

$$\mathbf{N} + \mathbf{L} = \mathbf{j} \qquad \mathbf{j} + \mathbf{S} = \mathscr{J}. \quad (9)$$

This coupling scheme corresponds more closely to the actual physics of the collision. The anisotropy of the atom–molecule electrostatic potential strongly couples **N** with **L**, while, in the absence of magnetic interactions, the electronic spin **S** plays a spectator role. In the limit that the spin-doublet splitting is small compared with the spacing between rotational levels, which is almost always the case for $^2\Sigma^+$ ground states, in other words when the coupling between **N** and **S** is small, the Corey–McCourt recoupling scheme allows us to express the full spin-dependent T-matrix elements in terms of spin-independent T-matrix elements, namely[14]

$$T^{\mathscr{J}}_{JLN,J'L'N'} = (-1)^{J'-J+L-L'}[(2J+1)(2J'+1)]^{1/2} \times \sum_j \begin{Bmatrix} S & N & J \\ L & \mathscr{J} & j \end{Bmatrix} \begin{Bmatrix} S & N' & J' \\ L' & \mathscr{J} & j \end{Bmatrix} T^j_{NL,N'L'}, \quad (10)$$

where $\{:::\}$ denotes a $6j$ symbol.[28] The spin-independent T-matrix elements $T^j_{NL,N'L'}$ can be obtained[14] by solution of a set of close-coupled (CC) equations *entirely equivalent* to those which describe the collision of a molecule in a closed-shell $^1\Sigma$ electronic state with a closed-shell atom.[32,33] For a $^2\Sigma^+$ molecule, $S = 1/2$ in Eq. (10), so that the Corey–McCourt recoupling scheme allows the replacement of *one* set of CC equations, containing *two* channels ($J = N \pm 1/2$) for each pair of N and L indices, with *two* sets of equations (with $j = J \pm 1/2$), containing only *one* channel for each N,L pair. Since the computational effort varies as the cube of the number of equations,[34] this recoupling effectively reduces the computational effort by a factor of 4 over that required in the earlier[11,31] formulations of the collisions of a $^2\Sigma^+$ molecule with a closed-shell spherical atom. This is a significant reduction.

Unfortunately, even with this reduction in dimensionality, a full CC calculation for collisions of CaCl is impractical, due to the large number of contributing channels for this molecule with closely spaced rotational levels. Nevertheless, we expect that the quantum coupled-states (CS) approximation will be accurate for CaCl–Ar collisions at hyperthermal energy. This assertion is supported by our comparison[13] of CC and CS cross sections for collisions of NO($X\,^2\Pi$). The Corey–McCourt recoupling scheme [Eq. (9)] can also be applied in the CS limit; the spin-free CC T-matrix elements [Eq. (10)] can be expressed in terms of spin-free CS T-matrix elements, namely,

$$T^j_{NL,N'L'} = i^{L+L'-2\bar{L}}[(2L+1)(2L'+1)]^{1/2} \times \sum_\nu \begin{pmatrix} L & N & j \\ 0 & \nu & -\nu \end{pmatrix} \begin{pmatrix} L' & N' & j \\ 0 & \nu & -\nu \end{pmatrix} T^{\bar{L}\nu}_{N,N'}. \quad (11)$$

Here the CS T-matrix elements which appear on the right-hand-side are *identical* to those which would arise in the formulation of the collision of a molecule in a $^1\Sigma^+$ electronic state with a spherical atom,[20–22,35–38] with an interaction potential identical to that for the $^2\Sigma^+$-atom system in question. The degeneracy averaged cross sections in case (b) labeling are given by[14]

$$\sigma_{JN\to J'N'} = \frac{\pi}{k^2_{NJ}} \sum_{\bar{L}\nu\nu'\mu} [(2J'+1)(2\bar{L}+1)] \begin{pmatrix} S & N' & J' \\ -\nu-\mu & \nu & \mu \end{pmatrix} \times \begin{pmatrix} S & N & J \\ -\nu-\mu & \nu & \mu \end{pmatrix} \begin{pmatrix} S & N & J \\ -\nu'-\mu & \nu' & \mu \end{pmatrix} \times \begin{pmatrix} S & N & J \\ -\nu'-\mu & \nu' & \mu \end{pmatrix} T^{\bar{L}\nu'*}_{N,N'} T^{\bar{L}\nu}_{N,N'}. \quad (12)$$

The dimensionality reduction discussed in the preceding paragraph is equally valid within the CS approximation.[14]

III. SCATTERING CALCULATIONS

The interaction potential describing the collision of a spherical atom with a molecule in a $^2\Sigma$ electronic state can be expanded in Legendre polynomials as[11,24]

$$V(R,\theta) = \sum_l v_l(R) P_l(\cos\theta), \tag{13}$$

where R is the distance between the atom and the center-of-mass of the molecule and θ is the angle between **R** and the molecular axis. In the present application $\theta = 0$ corresponds to the ClCa–Ar collinear configuration. The details of the potential surface have been described previously.[24] The electron-gas method of Gordon and Kim[23] was used to calculate[39] values of the CaCl–Ar potential $V(R,\theta)$ at 60 different geometries. Subsequently the R dependence, at fixed θ, was spline fit and the necessary $v_l(R)$ terms, at each R, were obtained by numerical quadrature. At long range the $l = 0$, 1, and 2 terms were smoothly joined to the corresponding induction and dispersion contributions. These latter were estimated with the Rittner model[40,41] used[24] to obtain the necessary electrostatic parameters for the CaCl molecule.

The scattering calculations were carried out using a new hybrid code,[42] which combines the log-derivative method (LOGD) of Johnson[43] at short range with, at long range, a variation (AIRY) of the original linear reference potential algorithm of Gordon,[34,44] designed to propagate directly the log-derivative matrix without determination of perturbation corrections. The code was adapted to run on a Floating Point Systems FPS-164 attached processor,[45] and full use was made of the FPS math library assembly language routines for the inversion, diagonalization, and multiplication of matrices.

The scattering calculations were carried out at a total energy of 1934 cm^{-1}, which corresponds to the average relative translational energy in the molecular beam experiment described in Sec. V. For a CS calculation at this energy there are 225 open rotational channels, since the rotational constant of CaCl is only 0.152 cm^{-1}.[46] As discussed in the preceding section, the Corey–McCourt recoupling scheme[14] replaces this 225 channel problem with two 113 channel problems ($N = 0$–112), which is still massive. The spin-free CS equations were solved for all even values of $\bar{L}$ [Eq. (12)] ranging from 0 to 600, beyond which point the inelastic transition probabilities become negligibly small. For convergence in the partial cross sections, even for low N and N', it was necessary to include all channels with $N = 0$–109 at small $\bar{L}$. The maximum value of N was progressively increased as $\bar{L}$ increased, so that only the $N = 0$–24 channels were included for $\bar{L} \geqslant 400$. The LOGD algorithm[43] was used to integrate the CS equations from a point 1 bohr inside the innermost classical turning point to a point 1.5 bohr outside the outermost turning point, typically a total distance of 3–4 bohr. The step size used was 0.025 bohr; typically ~ 150 LOGD steps were required. Subsequently, the AIRY algorithm[42] was used to integrate out to a final distance of 30 bohr; typically ~ 30 AIRY steps were required. The total computational effort was divided roughly equally between the two integrators. Calculations were carried out for values of the CS decoupling index ν in Eq. (12) of 0, 1, 2, 3, and 4. From the triangular relations contained in the 6j symbols in Eq. (10) and the 3j symbols in Eq. (11) this range of ν permits the determination of $J\epsilon \rightarrow J'\epsilon'$ cross sections for transitions with min $(J,J') \leqslant 9/2$. The complete set of scattering calculations required 115 h of CPU time on the FPS-164. For comparison purposes for a 49 channel calculation the LOGD integrator executes 14 times faster on the FPS-164 than on a VAX 11/780 (single precision) and the AIRY integrator, 20 times faster.

The calculated $J,\epsilon = 1 \rightarrow J'\epsilon'$ cross sections for $1/2 \leqslant J \leqslant 9/2$ and $1/2 \leqslant J' < 35/2$ are listed in Table I. We crudely estimate the precision of the tabulated cross sections to be ± 0.05 Å^2; the residual error reflects the choice of tolerance parameters in the numerical integration of the CS equations.[42] Within the energy sudden limit[47] the $J, -\epsilon \rightarrow J', -\epsilon'$ cross sections are predicted[11] to be identical to the $J\epsilon \rightarrow J'\epsilon'$ values. This identity was satisfied for all the cross sections computed, to well within the precision of the calculations. Thus, to save space only the cross sections out of the $\epsilon = +1$ levels (e levels) are listed in Table I.

IV. DISCUSSION OF CALCULATED CROSS SECTIONS

A. General behavior

We observe that substantial cross sections ($\geqslant 2$ Å^2) are predicted only for transitions involving small changes in the rotational quantum number ($\Delta J \leqslant 3$). Examination of the dependence on $\mathscr{J}$ of the degeneracy averaged partial cross sections, defined by

$$\sigma^{\mathscr{J}}_{J\epsilon \rightarrow J'\epsilon'} = \frac{\pi(2\mathscr{J}+1)}{k^2_{J\epsilon}(2J+1)} \sum_{L\bar{L}'} |T^{\mathscr{J}}_{J\bar{L}\epsilon,J'L'\epsilon'}|^2, \tag{14}$$

indicates that for these transitions there is a substantial contribution to the cross sections for values of $\mathscr{J}$ ranging from 200 to 600. For transitions involving large changes in the rotational quantum number ($\Delta J \geqslant 6$) the partial cross sections become negligibly small for $\mathscr{J} > 400$.

In a semiclassical description, $\mathscr{J} = 400$ corresponds to an impact parameter of 7.3 bohr. If we refer back to our description of the CaCl–Ar potential,[24] we observe that at a collision energy of 1934 cm^{-1} this impact parameter lies outside of the hard repulsive region of the potential except when the Ar atom approaches the Ca end of the CaCl molecule (see Fig. 1 of Ref. 24). Thus we can conclude that the ϵ-conserving cross sections for small ΔJ are significantly enhanced by grazing collisions involving interaction between Ar and the Ca^+ end of the CaCl molecule. The extended range of this interaction arises from the diffuse 4s electron on Ca^+ which is polarized away from the Cl^- ion. By contrast transitions with moderate to large changes in J arise entirely from direct interactions with the strong, anistropic repulsive wall in the potential surface.

B. Sudden scaling

The basically repulsive collision of the massive, slowly rotating CaCl molecule with Ar at a relatively high collision energy is most likely well described in the energy sudden limit.[47] If so, then the entire matrix of $J\epsilon \rightarrow J'\epsilon'$ cross sec-

TABLE I. Calculated $CaCl(X^2\Sigma^+) + Ar$ inelastic cross sections (Å^2); $E = 1934$ cm^{-1}.

			$\sigma_{J\epsilon=1\to J'\epsilon'(N=J-1/2,e\to N'e/f)}$[a,b]				
J'	ϵ'	N'[a]	$J=1/2$	3/2	5/2	7/2	9/2
1/2	1	0	154.8[c]	7.41	1.45	1.60	0.38
	−1	1	7.41	1.45	1.60	0.37	0.30
3/2	1	1	14.83	156.3[c]	10.18	2.13	2.33
	−1	2	2.90	4.37	1.06	1.03	0.46
5/2	1	2	4.35	15.26	156.9[c]	11.35	2.54
	−1	3	4.80	1.59	2.20	0.88	0.77
7/2	1	3	6.40	4.26	15.12	157.2[c]	12.00
	−1	4	1.50	2.06	1.17	1.41	0.70
9/2	1	4	1.88	5.82	4.24	14.98	157.6[c]
	−1	5	1.46	1.15	1.27	0.87	1.08
11/2	1	5	1.76	1.92	5.52	4.22	14.87
	−1	6	1.18	0.97	0.85	0.99	0.74
13/2	1	6	1.38	1.69	1.91	5.36	4.20
	−1	7	0.92	0.85	0.86	0.76	0.82
15/2	1	7	1.06	1.35	1.72	1.97	5.25
	−1	8	0.81	0.82	0.75	0.71	0.69
17/2	1	8	0.92	1.09	1.36	1.66	1.95
	−1	9	0.85	0.76	0.71	0.70	0.60
19/2	1	9	0.94	0.95	1.11	1.37	1.64
	−1	10	0.80	0.72	0.72	0.61	0.66
21/2	1	10	0.88	0.95	0.99	1.13	1.40
	−1	11	0.73	0.76	0.62	0.68	0.57
23/2	1	11	0.80	0.91	0.95	1.03	1.14
	−1	12	0.79	0.62	0.70	0.58	0.61
25/2	1	12	0.86	0.79	0.94	0.96	1.05
	−1	13	0.62	0.73	0.59	0.64	0.57
27/2	1	13	0.67	0.89	0.80	0.97	0.97
	−1	14	0.74	0.60	0.65	0.58	0.56
29/2	1	14	0.80	0.69	0.89	0.82	0.98
	−1	15	0.62	0.65	0.61	0.58	0.58
31/2	1	15	0.67	0.80	0.72	0.90	0.85
	−1	16	0.65	0.64	0.57	0.61	0.52
33/2	1	16	0.69	0.70	0.80	0.75	0.90
	−1	17	0.67	0.57	0.63	0.52	0.59
35/2	1	17	0.71	0.70	0.73	0.80	0.77

[a] In a case (b) labeling the e-labeled levels correspond to $N = J - 1/2$ and the f-labeled levels, to $N = J + 1/2$.
[b] We estimate the residual error in the tabulated cross sections to be ~ 0.05 Å^2, resulting primarily from residual numerical error in the integration of the coupled equations.
[c] The purely elastic cross sections are most likely lower bounds, since partial waves with $\mathcal{J} > 600$ will undoubtedly contribute.

tions can be interrelated by the sudden scaling relation[11]

$$\sigma_{J\epsilon\to J'\epsilon'} = (2J'+1)\sum_l (2l+1)\begin{pmatrix} J' & l & J \\ -1/2 & 0 & 1/2 \end{pmatrix}^2 \times \tfrac{1}{2}\left[1 - \epsilon\epsilon'(-1)^{J+J'+l}\right]\sigma_l, \quad (15)$$

where the "base" σ_l cross sections are proportional to cross sections for transitions out of the $J = 1/2$, $\epsilon = +1$ level, namely,[11]

$$\sigma_l = (l+1)^{-1}\,\sigma_{J=1/2,\epsilon=+1\to J'=l+1/2,\epsilon=+1}. \quad (16a)$$

or, alternatively, by microreversibility, to $J = l + 1/2$, $\epsilon = +1 \to J' = 1/2$, $\epsilon = +1$ cross sections, that is

$$\sigma_l = [(2l+1)/(2l+2)]\sigma_{J=l+1/2,\epsilon=+1\to J'=1/2,\epsilon=+1}. \quad (16b)$$

Equation (15) is the generalization to collisions of $^2\Sigma^+$ diatomics of a similar relation for collisions of $^1\Sigma^+$ molecules first derived by Goldflam, Green, and Kouri.[48,49] The reader should note that we have here removed the $(2l+1)$ factor from the definition of the σ_l cross sections, in contrast to our previous definition.[11]

If the initial and final nuclear rotation states are resolved, but not the spin doublets, then the overall cross section for an $N \to N'$ transition is obtained by summing over the four unresolved $J\epsilon \to J'\epsilon'$ transitions ($J = N \pm 1/2, J' = N' \pm 1/2$) weighted by the statistical weight associated with each initial value of J. These spin-unresolved cross sections can then, from Eq. (15), be written as[11]

$$\sigma_{N\to N'} = (2N'+1)\sum_l (2l+1)\begin{pmatrix} N' & l & N \\ 0 & 0 & 0 \end{pmatrix}^2 \sigma_l. \quad (17)$$

A comparison of Eqs. (15) and (17) reveals clearly the connection between the sudden scaling relations for collisions involving molecules in $^1\Sigma^+$ and $^2\Sigma^+$ electronic states. Note that the base cross sections are identical in Eqs. (15) and (17).

The full matrix of CS cross sections in Table I can be fit virtually exactly, with a root-mean-square deviation of 0.01 Å^2, by Eqs. (15) and (16). Thus CaCl–Ar collisions at an energy of 1934 cm^{-1} are well described by the sudden scaling relation.

A consequence of the applicability of the sudden scaling relation is the following equality:

$$\sigma_{J\epsilon \to J'\epsilon'} = \sigma_{J,-\epsilon \to J',-\epsilon'}. \tag{18}$$

which, as discussed at the end of Sec. III, implies that within a Hund's case (a) labeling, the cross sections will be unchanged under reversal of the e/f labeling of the initial and final states. It follows from Eq. (5) that within a Hund's case (b) labeling Eq. (18) implies the relations[11]

$$\sigma_{Ne \to Nf} = \sigma_{N+1,f \to N-1,e} \tag{19}$$

and

$$\sigma_{Ne \to N'e} = \sigma_{N+1,f \to N'+1,f}. \tag{20}$$

Equation (19) relates the transition across a particular spin doublet ($\Delta N = 0$) to a spin-changing transition with $\Delta N = 2$. Equation (20) implies that transitions within the e-labeled manifold are equivalent to transitions within the f-labeled manifold, but shifted down by one quantum of nuclear rotational angular momentum.

Another consequence of Eqs. (15) and (16) is that the cross sections for transitions into the $J = 1/2,e$ level can be related by

$$\sigma_{Je \to 1/2e} = \sigma_{J-1,f \to 1/2e}. \tag{21}$$

In a case (b) labeling, this equation becomes

$$\sigma_{Ne \to N=0} = \sigma_{Nf \to N=0}, \tag{22}$$

where we remember that only the e level exists for $N = 0$. Thus the cross sections for the two possible $N \to 0$ transitions are independent of the spectroscopic e/f label of the initial rotational level.

Because our calculated CS cross sections (Table I) are accurately described by the sudden scaling relation [Eq. (15)], Eqs. (19)–(22) are fully satisfied for CaCl–Ar collisions at $E = 1934$ cm^{-1}.

Since the calculated CS cross sections are well described by the sudden scaling relation, one naturally wonders whether it might be possible to use a sudden approximation, for example the infinite-order-sudden (IOS) method,[11,14,20,48–51] to calculate directly the CaCl($X\,^2\Sigma^+$)–Ar cross sections. This would certainly lead to a sizable reduction in computational effort. However, it will be first necessary to establish whether the accuracy of the sudden scaling relation is a sufficient condition for the accuracy of the IOS cross sections themselves.[52]

C. Fitting laws

In the interpretation of experimental studies of rotational energy transfer in excited $^1\Sigma^+$ electronic states of alkali dimers, Pritchard and co-workers have suggested[53–56] that the base cross sections in the sudden scaling relation [Eq. (17)] could be well fit by a simple power law

$$\sigma_l = a/[l(l+1)]^\gamma. \tag{23}$$

The original justification for this form was phenomenological, but was subsequently given support[55] by a simplistic treatment of the atom–molecule dynamics based on rectilinear trajectories. Recently, additional work[56,57] has been devoted to extensions of Eq. (23) to treat the case of collisions with light projectiles, where at large l experimentally determined base rate constants are observed to decrease faster than predicted by Eq. (23).[54,56,58]

The accuracy of Eq. (23) has been justified primarily by comparison with experimentally determined rate constants for collisional relaxation in electronically excited states and with the results of sudden-limit calculations.[59] An additional necessary test for the validity of the power law form, which has not yet been carried out, is the comparison with accurate quantum cross sections for the collision of a slowly rotating molecule with a heavy projectile under sudden conditions. The present set of theoretical cross sections allow us to make this comparison. The CS σ_l, defined by Eq. (16), are plotted in Fig. 1 for $1 \leqslant l \leqslant 55$. Due to the small rotational constant for CaCl($X\,^2\Sigma^+$), the rotational energy gap for even the $J = 0.5 \to J' = 55.5$ transition is only 465 cm^{-1}, less than 25% of the total collision energy, well within an energy sudden limit for a repulsive potential.

As can be seen in Fig. 1 there is considerable curvature in the log–log plot of the base cross sections, which indicates that a power law is an overly simplistic description of the collision. Note that the curvature is in the opposite sense to that observed previously in experimental studies involving collisions of electronically excited diatomics with light projectiles.[54,56,58] The major region of curvature is confined to low values of l, which corresponds to the largest values of the base cross sections. As can be seen in Fig. 1, at larger l ($l > 10$) the base cross sections can be fit well by a power law, to within the numerical accuracy of the calculated cross sections. The fit value of γ, 0.641, is significantly smaller than unity, the value derived from an analysis of Na_2^* collisions and predicted by a simplistic treatment of the collision dy-

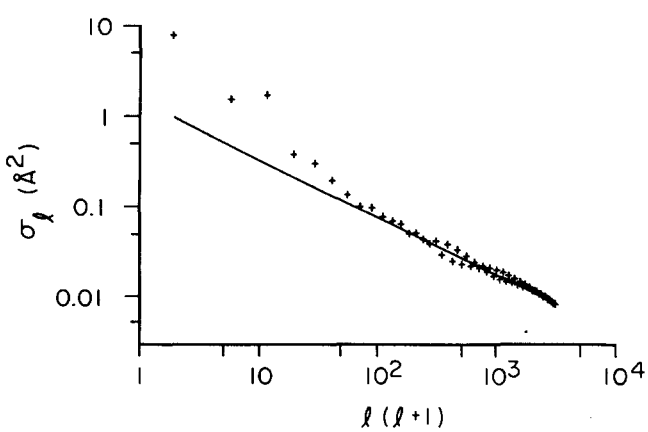

FIG. 1. Base CaCl($X\,^2\Sigma^+$)–Ar cross sections σ_l [Eq. (16)] from CS cross sections at $E = 1934$ cm^{-1}, plotted against $l(l+1)$. The straight line is a linear least squares fit to a power law form [Eq. (23)], which incorporates all base cross sections with $10 \leqslant l \leqslant 55$. The corresponding parameters are $a = 1.455$ Å^2 and $\gamma = 0.6405$.

namics,[55] but is comparable to the fitted exponent of Li_2^*–light projectile collisions, after correction for angular momentum constraints.[58]

We have here attempted to fit the large l base cross sections to a power law. Alternatively one could fit the small l values, and thereby obtain different values of a and γ in Eq. (23). It is clear from Fig. 1, however, that it is impossible to fit the *entire* set of base cross sections to Eq. (23).

It is important to stress that although the base cross sections for $l \geqslant 10$ can be fit well by a power law, there unfortunately exists no known way for *predicting accurately* the values of a and γ in Eq. (23) directly from the potential surface *without first carrying out the scattering calculation.* Thus, although there is clearly some physical content in these parameters, the relation with the potential surface is as yet obscure. Furthermore, the large, low-l base cross sections, which govern the experimentally accessible transitions (see Sec. V), are not well described by a simple power law.

D. Propensity rules

In our previous formal discussion of collisions involving molecules in $^2\Sigma^+$ electronic states, we used the large-J limit[28] of the $3j$ symbol appearing in the sudden scaling relation [Eq. (15)] to demonstrate that for a given J,J' pair the ϵ-changing (e/f changing) cross sections would be expected to become vanishingly small compared to the ϵ-conserving cross sections. This general propensity will become increasingly strong as both J and J' become large and $\Delta J = |J - J'|$ is small. This propensity was first seen experimentally in experiments by Lengel and Crosley[17] on OH($A\,^2\Sigma^+$) and has been confirmed by work by Dagdigian and Bullman[5,6] on collisions of CaCl($X\,^2\Sigma^+$) with molecular targets. The present set of theoretical CaCl($X\,^2\Sigma^+$) + Ar cross sections provides further confirmation. This is illustrated by Fig. 2(a), in which we plot the ratio of the e/f-changing to e/f-conserving cross sections for all $J \rightarrow J + \Delta J$ transitions with $1/2 \leqslant J \leqslant 9/2$ and $1 \leqslant \Delta J \leqslant 5$. The ratio decreases with increasing J and, overall, with decreasing ΔJ, as expected. Although the derivation of this propensity rule depends on a high-J limit[28] of the $3j$ symbol in Eq. (15), we observe that it is clearly apparent even for $\min(J,J') = 3/2$.

A similar propensity toward conservation of the e/f label also applies within a case (b) labeling, for transitions between rotational levels characterized by particular initial and final values of N, the nuclear rotational angular momentum. To show this we first use Eq. (5) to rewrite Eq. (15) as

$$\sigma_{Ne \rightarrow N'e/f} = (2N' + 1 \pm 1/2) \sum_l (2l + 1) \times \begin{pmatrix} N' & \pm 1/2 & l & N + 1/2 \\ & -1/2 & 0 & 1/2 \end{pmatrix}^2 \times \tfrac{1}{2}[1 + (-1)^{N+N'+l}]\sigma_l, \quad (24)$$

where the $+$ sign applies to e-labeled final states and the $-$ sign, to f-labeled final states. Note that the *same* l values contribute to *both* the $e \rightarrow e$ and $e \rightarrow f$ transitions, in contrast to the case (a) labeled description where for a given J and J' with $\Delta J =$ even, only odd l will contribute to the $e \rightarrow e$ transition and even l to the $e \rightarrow f$ transition. (This assignment is reversed for $\Delta J =$ odd.) Returning to Eq. (24), we observe that the phase factor inside the summation implies that for a given N,N' pair only those l values for which $(N + N' + l)$ is even will contribute. Now, the asymptotic development given in Eqs. (55)–(57) of Ref. 11 can be used here to demonstrate that with this constraint on $(N + N' + l)$ the $3j$ symbol will become asymptotically small in the case of the $-$ sign ($e \rightarrow f$ transitions) but not in the case of the $+$ sign ($e \rightarrow e$ transitions).

As stated in terms of case (b) labeling this propensity rule corresponds to the physical interpretation given earlier: Collisions governed by a purely electrostatic interaction do not affect the orientation of **S**, so that the relative orientation of **S** and **N**, which distinguishes the e and f levels,[6,11,25] tends to be conserved during the collision.[6,11,17] The propensity toward conservation of the e/f label within a case (b) labeling is confirmed by the present set of CaCl($X\,^2\Sigma^+$) + Ar cross sections, as illustrated by Fig. 2(b), in which we plot the ratio of the $e \rightarrow f$ to $e \rightarrow e$ cross sections for all $N \rightarrow N + \Delta N$ with $0 \leqslant N \leqslant 4$ and $1 \leqslant \Delta N \leqslant 5$. The ratio decreases with increasing N and, overall, with decreasing ΔN, as expected.

V. EXPERIMENTAL MEASUREMENTS OF CROSS SECTIONS

The experimental apparatus and technique for determining CaCl state-to-state rotationally inelastic cross sec-

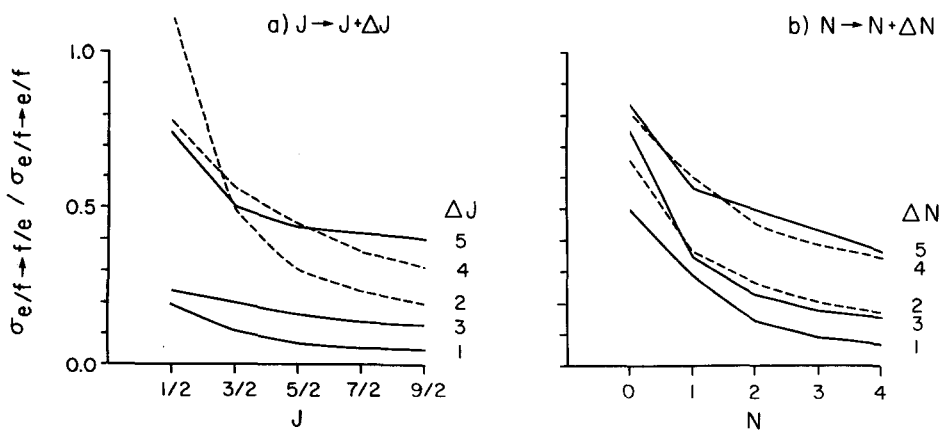

FIG. 2. (a) Ratio of e/f changing to e/f conserving $J \rightarrow J + \Delta J$ cross sections (Table I), as a function of J and ΔJ. (b) Ratio of e/f changing to e/f conserving $N \rightarrow N + \Delta N$ cross sections (Table I), as a function of N and ΔN. For clarity dashed lines are used to indicate the cross sections for transitions with ΔJ or ΔN even.

tions have been described in detail previously.[6] A supersonic beam containing CaCl is generated by vaporizing a mixture of calcium metal and anhydrous calcium dichloride heated to approximately 1260 K in a stainless crucible, and then expanding the gas through a 0.25 mm orifice maintained at a slightly higher temperature (1490 K) than the molten charge. The dominant species in the gas mixture is Ca atoms, which internally cool and accelerate the CaCl molecules.

After three stages of differential pumping the beam passes through a 1.0 mm diam collimator and is rotationally state selected by a 92 cm long electric quadrupole field (inside diam 9.5 mm). To prevent high J undeflected molecules from passing into the scattering chamber, the molecules are deflected through an annular obstacle (inner diam 2.4 mm, outer diam 6.7 mm) placed at the center of the quadrupole. The state-selected molecules pass through a 0.6 mm diam collimator into the scattering chamber. The quadrupole voltage was adjusted to select the $N = 2,e$ level. From the optimum refocusing voltage, the most probable CaCl velocity is estimated to be $(1.16 \pm 0.05) \times 10^5$ cm/s. As discussed in more detail earlier,[6] the principal impurities in the incident beam are the $N = 1,e$ and $N = 3,e$ levels (3%–5% each) and the $N = 2,f$ level, which is present (measured at line center[60]) at 8%–12% of the $N = 2,e$ refocused population.

State-selective detection is accomplished by fluorescence excitation in the CaCl $B\,^2\Sigma^+$–$X\,^2\Sigma^+$ band system with a single-mode cw dye laser. An additional laser fluorescence detector before the electric quadrupole is utilized to facilitate the initial setup of the experiment and to provide a strong fluorescence signal with which to lock the dye laser onto the center of a given CaCl line. Frequency stabilization is accomplished by modulation of the laser frequency using the external scan input of the dye laser. A drift correction voltage is derived by phase-sensitive detection of the locking signal and added to the external scan input.[60] In this way the dye laser can remain in the center of the nearly Doppler-free CaCl lines (50 MHz linewidth, due to natural broadening and unresolved hyperfine structure[61]) for hours. The dye laser beams were attenuated so as to avoid saturation effects.

The inelastic scattering experiments were carried out in the beam-gas configuration. The populations of the initially selected and collisionally populated final rotational levels are determined as a function of argon scattering gas pressure at a distance $l = 1.8 \pm 0.1$ cm downstream of the last collimator. The pressure is measured with a capacitance manometer to an accuracy of $\sim 5\%$, according to the manufacturer's specifications. This is consistent with the fact that two identical units in our laboratory recorded pressures differing by only $\sim 4\%$.

Under conditions of high incident state purity and low beam attenuation, the pressure dependence of the final to initial state population ratio follows the simple form[6,62]

$$n_f/n_i - n_f^{(0)}/n_i^{(0)} = n\sigma_{i\to f}l, \tag{25}$$

where n is the scattering gas density, $\sigma_{i\to f}$ is a state-to-state collision cross section, and the superscript (0) denotes populations at zero pressure. Equation (25) was employed to determine CaCl–Ar inelastic cross sections. The pressure dependence of the populations, as monitored by fluorescence intensities, was recorded with the aid of a microcomputer for the initial and a number of possible final states. In the Appendix we discuss in detail the line strength factors relating intensities to populations. The mixing of the $B\,^2\Sigma^+$ and $A\,^2\Pi$ states[63] significantly affects the ratio of the line strength factors for the R_1 and R_2 branches, which we have employed to monitor the e and f level populations, respectively.

Since the gas density is measured absolutely, the measured cross sections are absolute quantities. However, these are, strictly speaking, lower limits to the integral state-to-state cross sections since the detector only registers collisions in which the CaCl molecules are scattered into the forward laboratory direction. For the dipole–dipole systems previously studied,[5,6] the attenuation cross section equaled the sum of the inelastic cross sections so that the measured $\sigma_{i\to f}$ values could be equated with integral cross sections. In the present case, the measured state-to-state cross sections could underestimate the true integral cross sections if there were significant backward inelastic scattering in the laboratory frame. Finally, no correction to the populations needs to be made for the density-to-flux conversion[64] because the molecules are predominantly scattered forward with little change in relative translational energy.

Table II presents the experimentally determined $Ca^{35}Cl$–Ar state-to-state rotationally inelastic cross sections. The $e \to f$ cross sections are listed as upper limits because of the significant $N = 2,f$ impurity in the incident beam and the expected small magnitude of $e \to f$, as compared to $f \to f$, collisional transitions. The quoted collision energy was calculated by convoluting[65] the CaCl beam and Ar target gas velocity distributions.

VI. COMPARISON OF THEORY AND EXPERIMENT

Table II presents a comparison of the experimentally measured and theoretical (CS) cross sections for transitions out of the $N = 2,e$ ($J = 5/2,e$) level. We observe first that for the $e \to e$ transitions with $\Delta N =$ odd the theoretical and experimental cross sections agree consistently to within experimental error. This suggests that the experimental results do not seriously underestimate the integral cross sections. The situation is, however, different for the transitions with

TABLE II. Comparison of experimental and theoretical cross sections (Å^2) for collisions of CaCl with Ar; $E = 0.24$ eV (1934 cm^{-1}); initial level $N = 2,e$.

	Experiment		Theory[a]		Sudden fit[c]	
N'	e	f	e	f	e	f
0	4.0 ± 0.4		1.5		4.4	
1	9.4 ± 0.8		10.2	1.6	10.1	1.5
2	. . .		. . .	1.1	. . .	2.3
3	16.0 ± 1.3	$< 3.2 \pm 0.4$[b]	15.1	2.2	15.1	2.5
4	13.1 ± 1.1	$< 1.5 \pm 0.3$[b]	4.2	1.2	11.6	1.9
5	5.0 ± 0.5	$< 0.9 \pm 0.2$[b]	5.5	1.3	5.2	0.9
6	2.7 ± 0.3		1.9	0.9	2.7	0.5
7	1.8 ± 0.2		1.7	0.9	1.9	0.2
8	1.0 ± 0.2		1.4	0.8	0.9	0.1

[a] See Table I.
[b] Upper bound because of $N = 2,f$ impurity in incident beam.
[c] Predicted from sudden scaling relation [Eq. (15)] using base cross sections [Eq. (16), Table III] obtained by a least-squares fit to experimental cross sections given in columns 2 and 3.

ΔN = even, where the theoretical cross sections are consistently much smaller than the experimental values, particular for the two transitions with $\Delta N = 2$. For the experimentally measured $e \rightarrow f$ cross sections the agreement is acceptable, particularly in view of the fact that the experimental values for these transitions are only upper bounds. As in our previous studies of collisions of CaCl($X\,^2\Sigma^+$) with molecular targets,[5,6] the propensity toward conservation of the $e \rightarrow f$ label is pronounced.

The marked discrepancy between the experimental and theoretical cross sections for $\Delta N = 2$ certainly reflects a deficiency in the CaCl–Ar potential surface used here. Direct coupling between two rotational levels with the same e/f label and with ΔJ = even (ΔN = even) arises[11] from the even order Legendre terms in the atom–molecule potential [Eq. (13)]. Thus, in a perturbative model one could attribute directly the small values of the theoretical $\Delta N = 2$ cross sections to a deficiency in the description of the even moments of the anisotropy of the electrostatic interaction. Unfortunately, in an energy sudden limit, which we know to be appropriate here, this interpretation is simplistic, since a substantial contribution to the ΔN = even, $e \rightarrow e$ transitions can arise from the second order coupling involving the *odd* Legendre terms in the potential. Thus, it is unclear whether the discrepancy between the theoretical and experimental cross sections for $\Delta N = 2$ could be corrected by a simple enhancement of the $v_2(R)$ term [Eq. (13)] or whether it reflects a more complex interaction between the long- and short-range components in this term, or, in a more complicated manner, between these components and the $l = 1$ term. Although it would be too computationally expensive to use CS calculations to explore the sensitivity of the CaCl($X\,^2\Sigma^+$)–Ar cross sections to features of the potential surface, this type of study would be possible within the IOS approximation, should this prove to be accurate for this system.

Since the sudden scaling relation [Eq. (15)] describes well the matrix of calculated CS cross sections, it is reasonable to assume that it can fit equally well the experimental cross sections. If so, these latter values can be used to determine the fundamental set of base cross sections. To do so we carried out a linear least squares fit to the set of experimental values listed in Table II, to determine the set of σ_l which minimizes the reduced χ^2 error.[66] The procedure has been described elsewhere.[19] The number of l values used [Eq. (15)] was varied to minimize the reduced χ^2, subject to the constraints on the range of l imposed by the triangular relations in the $3j$ symbol in Eq. (15), and by the physical restriction that none of the resulting σ_l be negative. The values of σ_l obtained by this least squares fit are listed in Table III, and compared with the values calculated from the CS cross sections listed in Table I. We observe, as one might expect from the discussion in the preceding paragraph, that the low-l theoretical CS base cross sections all agree with the corresponding experimentally determined values to within the statistical error in the latter, except for $l = 2$ and $l = 4$, where the CS base cross sections are much smaller than the experimentally determined values. An indication of the accuracy of the sudden scaling relation is provided by the last two columns in Table II, where the base cross sections in Table III are used to predict the entire set of experimental cross sections for transitions out of the $N = 2,e$ level.

VII. CONCLUSION

In the present article we have investigated rotationally inelastic collisions of CaCl($X\,^2\Sigma^+$) with Ar at a collision energy of 0.24 eV. Theoretical cross sections, determined by coupled states calculations based on an electron-gas description of the interaction potential, were compared with experimental cross sections, determined in a molecular beam apparatus involving initial state selection by an electric quadrupole field and final state detection by laser-induced fluorescence. Our major conclusions are as follows:

(1) The agreement between the theoretical and experimental cross sections is excellent, except for the $e \rightarrow e$ transitions with ΔN = even, where the theoretical cross sections are substantially smaller than the experimental values. The overall agreement strongly suggests that the CaCl–Ar potential surface published previously[24] provides a globally accurate description of the size and anisotropy of the interaction, with some residual inaccuracy in the second Legendre moment of the anisotropy. The degree of agreement is very satisfying, in view of the crudeness of the electron-gas method used to calculate the interaction potential.

(2) Both the theoretical and experimental cross sections confirm the propensity toward conservation of the e/f label. Within a Hund's case (b) description of the rotational wave functions, this propensity is consistent with a dynamical model in which N changes in magnitude, while the relative orientation of N and S is preserved.[6] Our previous derivation[11] of this propensity rule within a case (a) description of the rotational levels, was extended here to a case (b) description.

(3) For the collisions of the massive, slowly rotating CaCl with Ar at a collision energy of 0.24 eV, the entire matrix of CS cross sections as well as the smaller set of experimental cross sections was found to be accurately represented by a sudden-limit scaling relation[11] in terms of a set of base cross sections. Comparison between the experimental and theoretical base cross sections indicated good agreement except for the $l = 2$ value, where the experimentally determined cross section was considerably larger than the corresponding theoretical value.

TABLE III. Base cross sections obtained by fit of experimental CaCl($X\,^2\Sigma^+$)–Ar cross sections to sudden scaling relation [Eq. (15)].[a]

l	σ_l(Å^2)[b]
1	7.44 ± 0.51 (7.42)
2	4.36 ± 0.30 (1.45)
3	1.45 ± 0.16 (1.60)
4	0.62 ± 0.08 (0.38)
5	0.44 ± 0.04 (0.29)
6	0.18 ± 0.04 (0.20)

[a] The reduced χ^2 (Ref. 66) corresponding to this fit is 1.9.
[b] Equation (16); the indicated uncertainties result from a standard error analysis (Ref. 66, Eq. (6–18)]. For comparison the theoretical values obtained from Table I and Eq. (16) are given in parenthesis.

(4) The present CS calculations, involving over 100 coupled channels, make possible a critical test of the power law fitting of the sudden limit base cross sections, advocated by Pritchard and co-workers.[53–56] Such a fit was found to adequately describe the set of base cross sections, but only if the large, experimentally relevant base cross sections are excluded from the set to be fit.

The theoretical calculations described here represent a substantial increase in computational difficulty over many previous studies of rotational energy transfer. This was made possible by the formal work of Corey and McCourt,[14] which permits the decoupling of the multiplicity in the rotational levels arising from the electronic spin, by the availability of a high-speed FPS-164 attached processor, and by the availability of a rapid new quantum scattering code.[42] The combination of these factors will certainly facilitate further quantum calculations of cross sections for collisions involving open-shell molecules. On the other hand, the accuracy of the sudden limit scaling relation strongly suggests that sudden limit dynamical approximations can be profitably used to calculate cross sections for collisions of nonhydride open-shell molecules[15] and to explore the dependence on the details of the potential surface. The advantage of the experimental technique described here, when compared to many other laser techniques,[17–19,54–58] is that collisions in an electronic ground state can be investigated. This facilitates the comparison with theory, since interaction potentials are easier to determine for ground state species. Only by future similar experimental work supplemented by related theoretical studies, can we hope to understand fully the collisional coupling between the relative nuclear motion of the collision partners and the various internal angular momenta (nuclear and electronic) of the target molecule.

ACKNOWLEDGMENTS

The research reported here was supported by the National Science Foundation under grants CHE84-00014 and CHE84–05828. The bulk of the scattering calculations were performed on the FPS-164 attached processor at the Center for Intensive Computation facility at the University of Maryland, supported, in part, by a grant to MHA by the U. S. Army Research Office under the DoD University Research Instrumentation Program (Grant DAAG-29-84-G-0078). Additional code development was supported by the Computer Science Center, University of Maryland and by the Academic Computing Services, George Mason University. The authors are grateful to Dr. Gregory Corey for his helpful comments on the manuscript and to Professor David Yarkony for information on the phase convention employed in the *ab initio* calculation of CaCl transition dipole matrix elements.

APPENDIX: FLUORESCENCE INTENSITY FACTORS FOR THE CaCl $B\,^2\Sigma^+$–$X\,^2\Sigma^+$ BAND SYSTEM

In this Appendix the intensity factors required for the conversion of CaCl $B\,^2\Sigma^+$–$X\,^2\Sigma^+$ fluorescence signals to $X\,^2\Sigma^+$ rotational populations are presented. We follow the general treatment of Greene and Zare (GZ)[67] and further assume that the M_J distributions of the detected molecules are isotropic. Thus, the fluorescence signal I for excitation from a level with total angular momentum J_i to an excited level J_e and subsequent emission to ground state level J_f is given by Eq. (13) of GZ, namely,

$$I = Cn_{J_i}\frac{S_aS_d}{3(2J_i+1)}\left[\frac{1}{3(2J_e+1)} + 2(-1)^{J_i-J_f} \times \begin{Bmatrix} J_e & J_e & 2 \\ 1 & 1 & J_f \end{Bmatrix}\begin{Bmatrix} J_e & J_e & 2 \\ 1 & 1 & J_i \end{Bmatrix} P_2(\cos\chi_{ad})\right]. \quad \text{(A1)}$$

Here n_{J_i} is the total population of the probed level; S_a and S_d are rotational line strengths for the absorption and emission processes, respectively; χ_{ad} is the angle between the absorption and detection polarization axes; and C is a proportionality constant including such factors as laser power, detector sensitivity, etc. In our apparatus, the fluorescence is not spectrally resolved and is observed with no polarization discrimination. Thus, we need to sum Eq. (A1) over J_f and two orthogonal detector polarization directions.

In the absence of any perturbations in the $X\,^2\Sigma^+$ and $B\,^2\Sigma^+$ states, both rotational line strengths S_a and S_d are given by the usual Hönl–London factors[25,68]:

$$S = (2J'+1)(2J+1)\begin{pmatrix} J' & 1 & J \\ 1/2 & 0 & -1/2 \end{pmatrix}^2, \quad \text{(A2)}$$

where J and J' are appropriate ground and excited state total angular momenta, respectively. However, the large value of the spin rotation constant γ of the $B\,^2\Sigma^+$ state indicates that this state is mixed to some extent with the $A\,^2\Pi$ state.[63] This mixing manifests itself in anomalous intensities, as has been observed in the SrF $B\,^2\Sigma^+$–$X\,^2\Sigma^+$ band system.[69]

In a treatment akin to that given by Nakagawa and Harris,[69] we express a perturbed wave function in the $B\,^2\Sigma^+$ state as

$$\psi = C_\Sigma|\Sigma\rangle + C_{\Pi_{1/2}}|\Pi_{1/2}\rangle + C_{\Pi_{3/2}}|\Pi_{3/2}\rangle, \quad \text{(A3)}$$

where the kets represents the unperturbed (Born–Oppenheimer) wave functions. We consider mixing only between the same vibrational levels of the $B\,^2\Sigma^+$ and $A\,^2\Pi$ states. This is permissible because the Franck–Condon factor array is very diagonal.

Considerable care must be taken to ensure the phase conventions for the Hamiltonian and the dipole matrix elements are consistent. We employ the convention of Larsson.[27] Thus, the matrix elements of the rotational and spin-orbit Hamiltonian, evaluated by the technique of Brown and Howard,[70] are

$$\begin{aligned}
&\langle\Sigma|H|\Sigma\rangle = T_\Sigma + B_\Sigma(J+1/2)(J+3/2),\\
&\langle\Pi_{1/2}|H|\Pi_{1/2}\rangle = T_\Pi - \tfrac{1}{2}A_\Pi + B_\Pi\left[J(J+1)+\tfrac{1}{4}\right],\\
&\langle\Pi_{3/2}|H|\Pi_{3/2}\rangle = T_\Pi + \tfrac{1}{2}A_\Pi + B_\Pi\left[J(J+1)-\tfrac{7}{4}\right],\\
&\langle\Pi_{1/2}|H|\Pi_{3/2}\rangle = -B_\Pi\left[(J-\tfrac{1}{2})(J+\tfrac{3}{2})\right]^{1/2},\\
&\langle\Sigma|H|\Pi_{1/2}\rangle = \xi + \eta\left[1-\epsilon(J+\tfrac{1}{2})\right],\\
&\langle\Sigma|H|\Pi_{3/2}\rangle = -\eta\left[J(J+1)-\tfrac{3}{4}\right]^{1/2}.
\end{aligned} \quad \text{(A4)}$$

Here T_Π, B_Π, and A_Π are the electronic energy, rotational constant, and spin-orbit constant for the A state, while T_Σ and B_Σ represent analogous quantities for the B state. The symmetry index ϵ is defined in Sec. II.

TABLE IV. Line strength factors[a] for $B\,^2\Sigma^+$–$X\,^2\Sigma^+$ laser fluorescence detection of CaCl $X\,^2\Sigma^+$ rotational populations.

	Unperturbed wave functions[b]		Including $B\,^2\Sigma^+$–A $^2\Pi$ mixing[c]	
N_i	R_1	R_2	R_1	R_2
0	1.175		1.175	
1	1.052	1.175	1.052	0.933
2	(1.000)	1.052	(1.000)	0.835
3	0.971	1.000	0.971	0.794
4	0.953	0.971	0.953	0.771
5	0.940	0.953	0.940	0.756
6	0.929	0.940	0.929	0.746
7	0.924	0.929	0.924	0.737
8	0.920	0.924	0.920	0.734

[a] Equation (A1) summed over J_f and orthogonal detector polarization directions. The probe laser polarization direction χ_a [see Fig. 2(a) of Ref. 67] equals 30° in our experiment. The line strength factors are normalized to unity for the $R_1(2)$ line.
[b] Rotational line strengths S given by Eq. (A2).
[c] Rotational line strengths S given by Eq. (A7).

The factors ξ and η are non-Born–Oppenheimer mixing parameters and are defined as[71]

$$\xi = \langle A\Lambda = +1|AL_+/2|B\Lambda = 0\rangle, \tag{A5}$$

$$\eta = \langle A\Lambda = +1|BL_+|B\Lambda = 0\rangle. \tag{A6}$$

These are approximated as $\xi = \frac{1}{2}A_\Pi\langle\Lambda = +1|L_+|\Lambda = 0\rangle$ and $\eta = B_\Pi\langle\Lambda = +1|L_+|\Lambda = 0\rangle$. The matrix element of L_+ is evaluated in the pure precession limit[25] as $2^{1/2}$. At the low values of J of interest in this experiment, the J-independent spin-orbit term in Eq. (A4) is the dominant cause of mixing, and the mixing coefficients are nearly independent of J. Typical values (taken for the $N=2$,e level) are $C_\Sigma = 0.9979$, $C_{\Pi_{1/2}} = 0.0655$, $C_{\Pi_{3/2}} = -4\times10^{-5}$.

The perturbed rotational line strength can be written as

$$S = (2J'+1)(2J+1)\left|C_\Sigma\begin{pmatrix} J' & 1 & J \\ 1/2 & 0 & -1/2\end{pmatrix} + (\mu_\perp/\mu_\parallel)\left[\epsilon C_{\Pi_{1/2}}\begin{pmatrix} J' & 1 & J \\ 1/2 & -1 & 1/2\end{pmatrix} - C_{\Pi_{3/2}}\begin{pmatrix} J' & 1 & J \\ 3/2 & -1 & -1/2\end{pmatrix}\right]\right|^2, \tag{A7}$$

where

$$\mu_\parallel = \langle B\Lambda = 0|\mu_0|X\Lambda = 0\rangle, \tag{A8}$$

$$\mu_\perp = \langle A\Lambda = -1|\mu_{-1}|X\Lambda = 0\rangle. \tag{A9}$$

Here μ_i denotes the spherical tensor components[28] of the electric dipole operator. The quantities $\mu_\parallel$ and $\mu_\perp$ have been determined in an *ab initio* MCSCF/CI calculation[72] to be $\mu_\parallel = 1.85$ a.u. and $\mu_\perp = 2.32$ a.u. at $R = 4.75$ bohr (near the calculated R_e value); hence, $\mu_\perp/\mu_\parallel = +1.26$.

Because the sign of ϵ is reversed for e and f levels, we find that the ratio of the R_2 to R_1 branch line strength factors is depressed by 26% over the ratio calculated using Eq. (A2). This factor has been taken into account here in converting fluorescence intensities to populations. The previously reported[5,6] cross sections for all f-labeled final states should be uniformly increased by 26%. As noted by Nakagawa and Harris,[69] the ratio of $R_1 + P_1$ to $R_2 + P_2$ intensities is unaffected by the perturbation. However, it was not convenient here to observe both R and P branches. In Table IV, we present the calculated line strength factors appropriate to our experimental configuration, determined both ignoring and including the effects of the $B\,^2\Sigma^+$–$A\,^2\Pi$ mixing. We note that the R_1 and R_2 branches detect the e and f levels, respectively.

[1] A. S. Sudbø and M. M. T. Loy, J. Chem. Phys. **76**, 3646 (1982).
[2] P. Andresen, H. Joswig, H. Pauly, and R. Schinke, J. Chem. Phys. **77**, 2204 (1982).
[3] P. Andresen, D. Häusler, and H. W. Lülf, J. Chem. Phys. **81**, 571 (1984).
[4] R. Copeland and D. Crosley, J. Chem. Phys. **81**, 6400 (1984).
[5] S. J. Bullman and P. J. Dagdigian, J. Chem. Phys. **81**, 3347 (1984).
[6] P. J. Dagdigian and S. J. Bullman, J. Chem. Phys. **82**, 1341 (1985).
[7] R. N. Dixon and D. Field, Proc. R Soc. London Ser. A **368**, 99 (1979).
[8] M. Shapiro and H. Kaplan, J. Chem. Phys. **71**, 2182 (1979).
[9] D. P. Dewangan and D. R. Flower, J. Phys. B **14**, 2179 (1984); B **18**, L137 (1985).
[10] V. N. Ostrowsky and V. I. Ustimov, J. Phys. B **14**, 1139 (1981); **17**, 99 (1984).
[11] M. H. Alexander, J. Chem. Phys. **76**, 3637 (1982).
[12] M. H. Alexander, J. Chem. Phys. **76**, 5974 (1982); M. H. Alexander and S. L. Davis, *ibid.* **79**, 227 (1983); M. H. Alexander and P. J. Dagdigian, *ibid.* **79**, 302 (1982); M. H. Alexander and B. Pouilly, *ibid.* **79**, 1545 (1983).
[13] T. Orlikowski and M. H. Alexander, J. Chem. Phys. **79**, 6006 (1983).
[14] G. C. Corey and F. R. McCourt, J. Phys. Chem. **87**, 2723 (1983).
[15] G. C. Corey, J. Chem. Phys. **81**, 2678 (1984).
[16] J. M. Brown, J. T. Hougen, K. P. Huber, J. W. C. Johns, I. Kopp, H.Lefebvre-Brion, A. J. Merer, D. A. Ramsay, J. Rostas, and R. N. Zare, J. Mol. Spectrosc. **55**, 500 (1975).
[17] R. K. Lengel and D. R. Crosley, J. Chem. Phys. **67**, 2085 (1977); D. Stepowski and M. J. Cottereau, *ibid.* **74**, 6674 (1981).
[18] O. Nédélec and J. Dufayard, Chem. Phys. **84**, 167 (1984).
[19] C. Dufour, B. Pinchemel, M. Douay, J. Schamps, and M. H. Alexander, Chem. Phys. (submitted).
[20] R. T Pack, J. Chem. Phys. **60**, 633 (1974).
[21] P. McGuire and D. J. Kouri, J. Chem. Phys. **60**,2488 (1974).
[22] D. J. Kouri, in *Atom–Molecule Collision Theory: A Guide for the Experimentalist*, edited by R. R. Bernstein (Plenum, New York, 1979), p. 301.
[23] R. G. Gordon and Y. S. Kim, J. Chem. Phys. **56**, 3122 (1972).
[24] S. L. Davis, B. Pouilly, and M. H. Alexander, Chem. Phys. **91**, 81 (1984).
[25] G. Herzberg, *Molecular Spectra and Molecular Structure. I. Spectra of Diatomic Molecules*, 2nd ed. (Van Nostrand, Princeton, 1950).
[26] R. N. Zare, A. L. Schmeltekopf, W. J. Harrop, and D. L. Albritton, J. Mol. Spectrosc. **46**, 37 (1973).
[27] M. Larsson, Phys. Scr. **23**, 835 (1981).
[28] D. M. Brink and G. R. Satchler, *Angular Momentum*, 2nd ed. (Oxford University, Oxford, England, 1975).
[29] See Appendix B of M. H. Alexander and P. J. Dagdigian, J. Chem. Phys. **80**, 4325 (1984).
[30] This expression has been corrected from Ref. 11 which made use of an erroneous expression for the parity of the spin eigenfunctions in Ref. 26, as discussed by Larsson (Ref. 27).
[31] R. N. Dixon and D. Field, Proc. R. Soc. London Ser. A **366**, 225 (1979).
[32] D. Secrest, in *Atom–Molecule Collision Theory: A Guide for the Experimentalist*, edited by R. B. Bernstein (Plenum, New York, 1979), p. 265.
[33] W. A. Lester, Jr., Methods Comput. Phys. **10**, 211 (1971).
[34] R. G. Gordon, Methods Comput. Phys. **10**, 81 (1971).
[35] M. Tamir and M. Shapiro, Chem. Phys. Lett. **31**, 166 (1975); **35**, 79 (1976).
[36] P. McGuire, J. Chem. Phys. **65**, 3275 (1976).
[37] Y. Shimoni and D. J. Kouri, J. Chem. Phys. **66**, 2841 (1977).
[38] G. Parker and R. T Pack, J. Chem. Phys. **66**, 2850 (1977).
[39] S. Green and R. G. Gordon, program POTLSURF, QCPE No. 251, University of Indiana, Bloomington, IN 47405.
[40] E. S. Rittner, J. Chem. Phys. **19**, 1030 (1951).
[41] P. Brumer and M. Karplus, J. Chem. Phys. **58**, 3903 (1973).
[42] M. H. Alexander, J. Chem. Phys. **81**, 4510 (1984).
[43] B. R. Johnson, J. Comput. Phys. **13**, 445 (1973); *Proceedings of the NRCC Workshop on Algorithms and Computer Codes in Atomic and Molecular Scattering Theory*, edited by L. D. Thomas, Lawrence Berkeley Report LBL-9501 (Lawrence Berkeley, Berkeley, CA); **I**, 86 (1979); **II**, 52 (1980).

[44]R. G. Gordon, J. Chem. Phys. **51**, 14 (1969).
[45]See, for example, R. Shepard, R. A. Bair, R. A. Eades, A. F. Wagner, M. J. Davis, L. B. Harding, and T. H. Dunning, Jr., Int. J. Quantum Chem. **17**, 613 (1983).
[46]K. P. Huber and G. Herzberg, *Molecular Spectra and Molecular Structure. IV. Constants of Diatomic Molecules* (Van Nostrand, New York, 1979).
[47]V. Khare, J. Chem. Phys. **68**, 4631 (1978).
[48]R. Goldflam, S. Green, and D. J. Kouri, J. Chem. Phys. **67**, 4149 (1977).
[49]R. Goldflam, D. J. Kouri, and S. Green, J. Chem. Phys. **67**, 5661 (1977).
[50]D. Secrest, J. Chem. Phys. **62**, 710 (1975).
[51]L. W. Hunter, J. Chem. Phys. **62**, 2855 (1975).
[52]See, for example, E. F. Jendrek and M. H. Alexander, J. Chem. Phys. **72**, 6452 (1980).
[53]T. A. Brunner and D. E. Pritchard, in *Dynamics of the Excited State*, edited by K. P. Lawley (Wiley, New York, 1982), p. 589, and references contained therein.
[54]T. P. Scott, N. Smith, and D. E. Pritchard, J. Chem. Phys. **80**, 4841 (1984).
[55]T. A. Brunner, T. P. Scott, and D. E. Pritchard, J. Chem. Phys. **76**, 5641 (1982).
[56]S. L. Dexheimer, M. Durand, T. A. Brunner, and D. E. Pritchard, J. Chem. Phys. **76**, 4996 (1982).
[57]B. Whitaker and P. Bréchignac, Chem. Phys. Lett. **95**, 407 (1983).
[58]J. Derouard and N. Sadeghi, J. Chem. Phys. **81**, 3002 (1984); Chem. Phys. **88**, 171 (1984).
[59]J. M. Bowman and S. C. Leasure, J. Chem. Phys. **66**, 288, 296 (1977).
[60]S. J. Bullman and P. J. Dagdigian, Chem. Phys. **88**, 479 (1984).
[61]W. J. Childs, D. R. Cok, and L. S. Goodman, J. Chem. Phys. **76**, 3993 (1982).
[62]P. J. Dagdigian, B. E. Wilcomb, and M. H. Alexander, J. Chem. Phys. **71**, 1670 (1979).
[63]L. E. Berg, L. Klynning, and H. Martin, Phys. Scr. **21**, 173 (1980).
[64]H. W. Cruse, P. J. Dagdigian, and R. N. Zare, Faraday Discuss. Chem. Soc. **55**, 277 (1973).
[65]L. Pasternack and P. J. Dagdigian, J. Chem. Phys. **67**, 3854 (1977); R. C. Estler and R. N. Zare, Chem. Phys. **28**, 253 (1978).
[66]P. R. Bevington, *Data Reduction and Error Analysis for the Physical Sciences* (McGraw–Hill, New York, 1969).
[67]C. H. Greene and R. N. Zare, J. Chem. Phys. **78**, 6741 (1983).
[68]R. N. Zare, in *Molecular Spectroscopy: Modern Research*, edited by K. N. Rao and C. W. Mathews (Academic, New York, 1972), p. 207.
[69]J. Nakagawa and D. O. Harris, J. Mol. Spectrosc. **86**, 65 (1981).
[70]J. M. Brown and B. J. Howard, Mol. Phys. **31**, 1517 (1976).
[71]See, for example, D. F. Reisner, P. F. Bernath, and R. W. Field, J. Mol. Spectrosc. **89**, 107 (1981). The right-hand side of Eq. (2a) should be multiplied by 2.
[72]N. Honjou, G. F. Adams, and D. R. Yarkony, J. Chem. Phys. **79**, 4376 (1983).